Chinese Chemical Letters 34 (2023) 108516

Contents lists available at ScienceDirect

Chinese Chemical Letters

journal homepage: www.elsevier.com/locate/cclet

A highly selective fluorescent probe for visualizing dry eye disease-associated viscosity variations

Lili Lian[a,c,1], Ruirui Zhang[b,1], Shuai Guo[a], Zhenmin Le[a,c], Lixiong Dai[d], Yueping Ren[a,c,*], Xiao-Qi Yu[b], Ji-Ting Hou[a,*], Jianliang Shen[a,d,*]

[a] National Engineering Research Center of Ophthalmology and Optometry, Eye Hospital, Wenzhou Medical University, Wenzhou 325027, China
[b] Key Laboratory of Green Chemistry and Technology (Ministry of Education), College of Chemistry, Sichuan University, Chengdu 610064, China
[c] National Clinical Research Center for Ocular Diseases, Eye Hospital, Wenzhou Medical University, Wenzhou 325027, China
[d] Wenzhou Institute, University of Chinese Academy of Sciences, Wenzhou 325000, China

ARTICLE INFO

Article history:
Received 7 March 2023
Revised 25 April 2023
Accepted 25 April 2023
Available online 27 April 2023

Keywords:
Fluorescent probe
Viscosity
Bioimaging
Corneal tissue
Dry eye disease

ABSTRACT

Dry eye disease (DED) is a multifactorial chronic inflammatory disease of the ocular surface with complex and unclear etiology. The development of reliable detection tools for the pathology of DED will benefit its treatment, but it is still lacking. In parallel, it has been discovered recently that viscosity changes are involved in inflammation processes. In this regard, we constructed a fluorescent probe **V5** with an asymmetric donor-acceptor-donor (D-A-D) feature after rational structural modulation for viscosity detection during DED progression. The probe manifested a remarkable fluorescence enhancement (110 folds) in highly viscous conditions without interferences from polarity and reactive species. Specifically, no aggregation effect of the probe was found in glycerol. Moreover, viscosity increment in human corneal epithelial cells (HCECs) induced by hyperosmosis and inflammation was monitored, and ferroptosis in HCECs also led to the viscosity elevation. A reactive oxygen species (ROS)-dependent viscosity changes during DED progression is demonstrated. Finally, viscosity change in corneal epithelial cell layer from mice treated by scopolamine was also visualized for the first time. We anticipate this work can provide a new lens to the pathogenesis study and diagnosis of DED and other ophthalmic diseases using fluorescence methods.

Intracellular microenvironments (viscosity, polarity, redox, *etc.*) have been verified to be tightly associated with cellular functions [1]. Among them, viscosity, as a key parameter of microenvironments, is heterogeneously distributed in the different regions in cells, ranging from 50–90 cP in lysosomes to 200–300 cP in membrane [2,3]. Regular viscosity is pivotal for maintaining normal biological processes such as membrane fusion and material transport [4,5]. In contrast, aberrant viscosity is closely related to pathological processes, like hepatic ischemia reperfusion injury, cardiovascular diseases, and tumors [6–8]. Therefore, the precise detection of viscosity changes in bio-systems is highly demanded for disease diagnosis.

To this end, fluorescence imaging technique has evolved into the leading tool to monitor cellular functions because of its high sensitivity, non-invasive operation, and pervasive facilities [9–18]. Over the past ten years, and especially in the last five, a mountain of fluorescent probes have been presented to showcase intracellular viscosity changes [2,6,19-44], and some of them have been successfully applied in various pathological processes, such as fatty liver, stroke, and ferroptosis [26-28,42]. A viscosity-responsive probe generally contains a rotor that can eliminate fluorescence of the probe due to motion-induced non radiative decay under low-viscosity condition; in highly viscous condition, the fluorescence of the probe can be recovered because of the inhibition of intramolecular motion, thereby realizing viscosity sensing. Compared with activity-based fluorescent probes for other biomarkers including enzymes and reactive oxygen species (ROS) [45–47], viscosity-responsive probes possess several unique advantages. First, since viscosity-responsive probes do not need additional reaction sites, they are more facile to synthesize. Second, activity-based fluorescent probes are commonly irreversible while viscosity-responsive probes are reversible, implying that the latter ones are more applicable to dynamically monitor the

* Corresponding authors.
E-mail addresses: yuepingren@aliyun.com (Y. Ren), houjiting2206@163.com (J.-T. Hou), shenjl@wiucas.ac.cn (J. Shen).
[1] These authors contributed equally to this work.

https://doi.org/10.1016/j.cclet.2023.108516
1001-8417/

progression of relevant pathological processes during a period of time. Therefore, viscosity-based fluorescent probes are of great potential for clinical disease diagnosis.

However, in spite of the achievement in viscosity detection, some drawbacks still exist in the fabrication of viscosity-based probes. First, since most of viscosity-responsive probes are polar molecules, they always suffer from solvent effects, and polarity is a common interference factor to induce false positive signals of these probes [48]. Second, viscosity-responsive probes usually contain reactive C=C bond to enlarge the π-conjugation, while this architecture enables them susceptible to ROS or reactive sulfur species (RSS) such as biothiols [46,49]. Third, molecules featured with aggregation-induced emission (AIE) are also employed for viscosity detection [50,51]. Nevertheless, their enhanced emission in cells can be ascribed to either viscosity elevation or the formation of aggregation. Therefore, an ideal viscosity-based probe should be stable without AIE effect, and its optical performance should not be affected by polarity, yet the above issues have not been inspected in most cases, and it is still challenging to develop a high-performance fluorescent probe for viscosity.

Dry eye disease (DED) is a multifactorial chronic inflammatory disease in the ocular surface, and its prevalence ranged from approximately 5% to 50% in different populations and regions [52]. DED causes visual disorders and corneal neurosensory abnormalities, reducing the life quality of patients and increasing their economic burden. Currently, there is no definitive therapeutic regimen for DED since the etiology is complicated and unclear [53]. Therefore, it is of great demand for developing new tools to reveal the pathology of DED. Recently, it has been discovered that abnormal intracellular microenvironments such as viscosity are closely associated with excessive inflammatory responses [19]. Therefore, monitoring viscosity changes during DED progression might serve as an alternative to its pathology inspection.

In this regard, we constructed a series of fluorescent probes for viscosity sensing, including two donor-acceptor (D-A) molecules **V1** and **V2** and four donor-acceptor-donor (D-A-D) molecules **V3**–**V6**. 2,6-Dimethyl pyridinium salt was chosen as the electron-withdrawing center, and triphenylamine (TPA) and phenothiazine (PTZ) as electron-donating segments. Among them, compound **V5** with an asymmetric D-A-D feature shows the most desirable sensing performance under viscous condition. It displays obvious fluorescence enhancement upon the increment of viscosity without interferences from polarity and reactive species. It can selectively discriminate cancer cells from normal ones owing to their inherent higher viscosity. Furthermore, the probe is employed to monitor viscosity variations in human corneal epithelial cells (HCECs) under different conditions to indicate DED pathology, including hyperosmosis (HO) and inflammation. Especially, the probe is successfully used for imaging corneal epithelial tissues from DED-modeled mice. To the best of our knowledge, **V5** is the first probe used for monitoring DED-associated viscosity. The synthetic route for **V1**–**V6** is illustrated in Scheme S1 (Supporting information), and they were fully characterized by ^{1}H nuclear Magnetic Resonance (NMR), ^{13}C NMR, and high-resolution mass spectrum (HRMS) (Supporting information).

In general, viscosity-responsive probes were prepared in a D-A type which is featured with strong intramolecular charge transfer (ICT) [19–23]. Such molecules usually emit fluorescence in highly viscous solvents such as glycerol and apolar solvents such as 1,4-dioxane, thus lacking selectivity to viscosity. Moreover, the number of rotors in D-A structures may not be sufficient for complete quenching of their fluorescence, leading to their limited sensitivity to viscosity. It is anticipated that increasing rotor numbers should amplify the sensitivity of viscosity-specific probes. To test this conjecture, two D-A and four D-A-D molecules were prepared with different kinds of donors and different numbers of molecular rotors (Scheme 1). Pyridinium salt is selected owing to its inherent mitochondrial targetability and excellent aqueous solubility. Different donors including TPA and PTZ units are attached in order to modulate the probes' optical behaviors in apolar solvents and glycerol. TPA is selected due to its intrinsic rotatable phenyls and PTZ displays vibratory characteristic. Both two donors have been utilized for sensing viscosity [23]. In addition, an asymmetric D-A-D structure **V6** with donors at 2–4 positions of pyridinium unit was manufactured.

Initially, the emission spectra of **V1**–**V6** in different solvents were investigated, including highly polar solvents (H_2O, dimethyl sulfoxide (DMSO), acetonitrile (MeCN), *N*,*N*′-dimethylformamide (DMF), methanol (MeOH)), weakly polar solvents (1,4-dioxane, tetrahydrofuran (THF), dichloromethane (DCM)), and viscous glycerol. As shown in Figs. 1A–F, almost all of the probes barely fluoresced in highly polar sol-vents, while their behaviors in weakly polar solvents and glycerol remarkably varied. In detail, D-A structure **V1** bearing one PTZ unit showed a distinct emission band at 627 nm in 1,4-dioxane and weak fluorescence in THF and glycerol. Similarly, D-A-D structure **V3** with two PTZ units exhibited strong fluorescence in 1,4-dioxane and THF. The results indicate that PTZ as donors tends to endow the probes with ability to sense polarity rather than viscosity. Furthermore, although **V2** with a common rotor TPA emitted an intensive fluorescence in glycerol, its intensities in 1,4-dioxane and THF were higher. By adding one more TPA head, a reverse optical behavior could be achieved in **V4** which displayed a strong emission band around 600 nm in glycerol, a moderate emission at 650 nm in DCM, and a weak emission at 590 nm

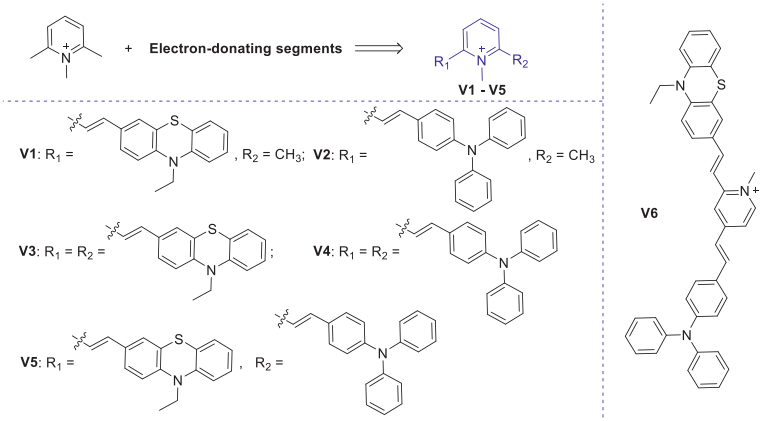

Scheme 1. Design of pyridinium-based probes **V1**–**V6**.

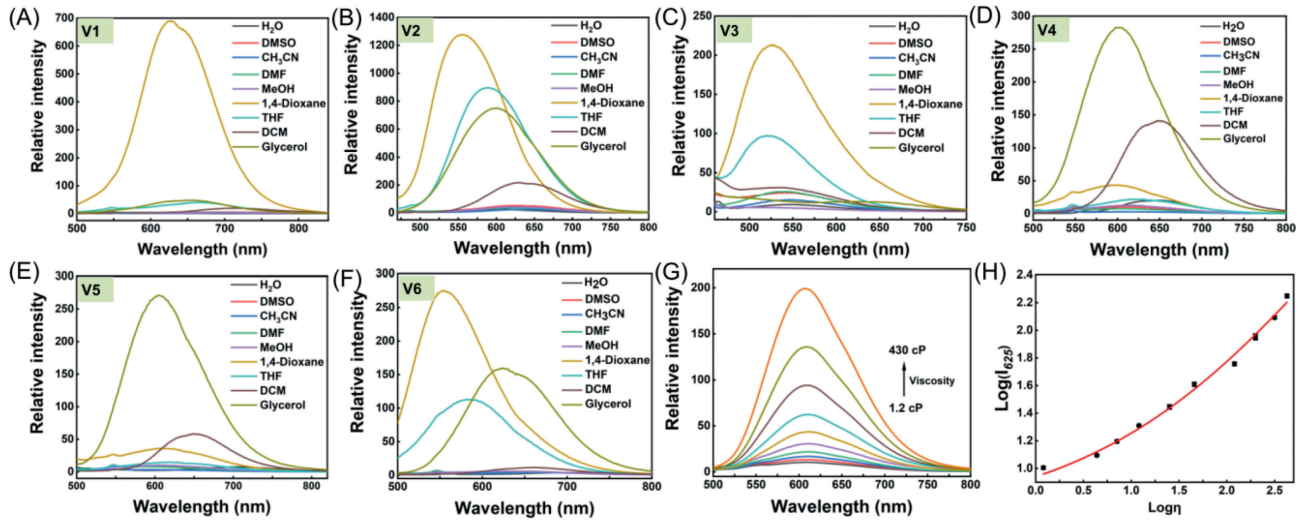

Fig. 1. The fluorescence spectra of (A–F) **V1**–**V6** (5 μmol/L) in different solvents. (G) The fluorescence spectra of **V5** (5 μmol/L) in methanol with increasing fractions of glycerol (0–90%). (H) The intensity changes at 605 nm plotted *vs.* viscosity value. λ_{ex} = 470 nm, slit: 5 nm/5 nm.

in 1,4-dioxane, suggesting that TPA is more preferable for viscosity sensing than PTZ and increasing rotor numbers can reliably amplify viscosity sensitivity. Interestingly, by replacing one TPA unit in **V4** with a PTZ moiety, a higher selectivity to viscosity over polarity was attained *via* an asymmetric D-A-D structure **V5**. **V5** apparently fluoresced at 605 nm in glycerol with a 110-fold intensity enhancement compared with that in water (Fig. S1 in Supporting information). However, as a positional isomer of **V5**, **V6** with donors at 2,4-positions displayed a strong emission at 556 nm in 1,4-dioxane and a less strong emission at 625 nm in glycerol, losing the selectivity. Overall, not all electron donors are suitable for constructing D-A type probes for viscosity, rotatable donors should be more favorable for construction of viscosity-responsive probes than vibratory ones, and D-A-D type molecules might be superior for viscosity sensing than D-A type owing to their more abundant rotors. In addition, the positions of donors around the acceptor center should be another key factor for improving the selectivity of probes.

After confirming the best sensing performance of **V5** toward viscosity, its optical behavior was further inspected. First, its absorption spectra in different solvents were examined. As shown in Fig. S2 (Supporting information), the maximum absorbance bands of the probe in the tested solvents primarily located in the range from 470 nm in 1,4-dioxane to 487 nm in glycerol, except that of 528 nm in DCM. It is of interest that a Tyndall effect was observed in H_2O under laser irradiation, indicating the formation of **V5** aggregates in water (Fig. S2). By contrast, no similar phenomenon was found in methanol and glycerol solutions, suggesting that the bright fluorescence of **V5** in glycerol originates from disperse unimolecules rather than aggregates. Moreover, in a viscous mixture of glycerol-methanol (1:1, v/v), the increment in maximum absorbance of **V5** at 485 nm followed the Lambert-Beer's law with its concentrations ranging from 1 μmol/L to 30 μmol/L and no shift in the maximum absorption wavelength was observed, excluding the aggregation of **V5** (Fig. S3 in Supporting information). Meanwhile, the fluorescence spectra of **V5** in THF with varying water fractions were recorded. It was found that increasing fractions of water in THF did not enhance the emission intensity of the probe (Fig. S4 in Supporting information). Thus, AIE effect could be excluded in the sensing process of **V5** toward viscosity.

Then, the fluorescence performance of **V5** in methanol upon increasing fractions of glycerol was explored. As shown in Figs. 1G and H, the probe barely fluoresced in methanol. Along with the increasing viscosity from 1.2 cP to 430 cP, the emission intensity at 605 nm was amplified apparently with quantum yields increasing from 0.88% in methanol to 7.66% in 90% glycerol, and no wavelength shift was observed. It was ascribed to the restriction of intramolecular motion of the probe by high viscosity which inhibited non-radiative decay. Considering that the probe is armed with two reactive C=C double bonds and one reductive PTZ unit, its chemostability was investigated in the presence of various ROS and RSS, including $^{\bullet}OH$, $O_2^{\bullet-}$, $ONOO^-$, ^tBuOOH, ClO^-, H_2O_2, S^{2-}, $S_2O_3^{2-}$, and SO_3^{2-}. As shown in Fig. S5 (Supporting information), the absorption and emission spectra of the probe showed negligible variations upon addition of these reactive species, suggesting the superb chemostability of **V5**.

It has been confirmed that the microenvironment in cancer cells is more viscous than that in normal cells [19]. To verify the applicability of the probe for bioimaging, two types of normal cell lines (RAW 264.7 and L929 cells) and two cancer cell lines (HeLa and A549 cells) were incubated with the probe for 20 min, respectively. As depicted in Fig. S6 (Supporting information), dim fluorescence was observed in normal cells while much brighter light (~3 folds) was captured in cancerous ones. The results validated the ability of the probe to monitor intracellular viscosity changes. Notably, the fluorescent spots in cancer cells were found to distribute out of nucleus. To further specify the intracellular localization of the probe, co-staining of **V5** in HeLa cells with commercial dyes was carried out, including Lyso Tracker Green (LTG) for lysosomes and Mito Tracker Green (MTG) for mitochondria. It was uncovered that the fluorescence signals from the probe were better overlapped with that from MTG, and the Pearson's coefficients were calculated to be 0.54 with LTG and 0.85 with MTG in several, suggesting that **V5** primarily located in mitochondria probably owing to its positive pyridinium fragment (Fig. S7 in Supporting information).

Viscosity changes in HeLa cells under various stimuli were then investigated. It has been reported that tunicamycin (TCY), dexamethasone (Dex), and nystatin (Nys) can induce viscosity upregulation in endoplasmic reticulum, lysosomes, and mitochondria, respectively [29,43,54]. HeLa cells were separately pre-incubated with these three drugs (10 μg/mL) before treatment with the probe. As exhibited in Fig. S8 (Supporting information), increasing fluorescence was observed in all groups of cells treated with viscosity inducers, suggesting that **V5** can image intracellular viscosity variations. In addition, the increment in fluorescence intensity from drug-treated cells followed the order: Nys > Dex > TCY (Fig. S8B),

indicating that **V5** can more sensitively detect mitochondrial viscosity changes, which is identical with the fact that **V5** is mainly accumulated in mitochondria. Afterwards, the dynamic viscosity changes in Nys-treated cells were monitored. HeLa cells were initially cultured with Nys (10 μg/mL) for different time (0, 1, 2, and 4 h). It was found that the fluorescence gradually increased along with the prolonged drug treatment time and reached a plateau after 2 h, implying that Nys could regulate mitochondrial viscosity within 2 h (Fig. S9 in Supporting information).

Although the etiology of DED is complex and unclear, mitochondrial dysfunctions are confirmed to be deeply involved in DED [55]. Therefore, the probe **V5** that can detect mitochondrial viscosity variations is expected to illustrate the DED progression. First, the cytotoxicity of the probe in HCECs was assessed. As shown in Fig. S10 (Supporting information), when HCECs were incubated with different concentrations of **V5** ranging from 0 to 10 μmol/L, the cell viability almost kept unchanged after 24 h Furthermore, the biosafety of **V5** was further inspected on C57BL/6J mice. All animal experiments were performed in accordance with the ARVO statement for the Use of Animals in Ophthalmic and Vision Research and the approved guidelines of the Wenzhou Medical University Institutional Animal Care and Ethics Committee. After being injected with the solution containing **V5** through the tail vein, the creatinine (CR), aminotransferase (GOT), alanine aminotransferase (GPT), and blood urea nitrogen (BUN) were detected by the commercially available kits. From Fig. S11 (Supporting information), it could be concluded that renal function and liver function were not affected after 24 h post-injection of **V5**. These results indicated the excellent biocompatibility of the probe.

Subsequently, the sensing performance of **V5** in during DED progression was evaluated. HO and inflammation are considered as core mechanisms for the occurrence of DED [56,57], thus, HCECs featured with high osmotic pressure (450 mOsm) were achieved by treatment with 70 mmol/L NaCl, and lipopolysaccharide (LPS) was used to induce inflammation. As shown in Fig. S12 (Supporting information), faint red fluorescence was observed in cells only treated with the probe, suggesting low viscosity in normal HCECs. In contrast, brighter fluorescence was visualized in cells with HO and inflammation symptoms, indicating that the mitochondrial viscosity in HCECs became higher as a result of the occurrence of the DED. Also, Nys was found to cause viscosity increment in HCECs, similar to HeLa cells.

Then, the time dependent viscosity changes during DED progression were investigated. HCECs were stimulated by high-concentration NaCl and LPS for 0, 2, 4, or 8 h, respectively, and then incubated with **V5** for another 20 min. As exhibited in Figs. 2A and B, gradually enhanced fluorescence was monitored in both cases along with the extended stimulation time, indicating elevated viscosity during the DED progression induced by HO or inflammation. As oxidative stress has been suggested to play a key role in the development of DED [55], we assumed that the viscosity-amplified conditions in the abnormal HCECs should be associated with ROS variations. To validate this hypothesis, NaCl- or LPS-pretreated HCECs were cultured with a commercial ROS probe CM-H2DCFDA. As depicted in Figs. 2C and D, overproduction of ROS was recorded in the cells with DED phenotype, and the rising tendency of ROS level resembled that of viscosity. Furthermore, in the HCECs which were successively treated with *N*-acetylcysteine (NAC, an antioxidant) and NaCl, both of the viscosity and ROS level decreased (Fig. S13 in Supporting information), affirming the tight correlation between viscosity and oxidative stress in mitochondria during DED progression. The results imply that **V5** can be used to indicate DED-associated viscosity changes.

Recently, it has been revealed that oxidative stress-mediated ferroptosis participates in the death of corneal epithelial cells DED [58], while the intracellular microenvironment changes during ferroptosis in HCECs has been rarely discussed. To elucidate this pathological process, HCECs were pretreated with (1*S*,3*R*)-methyl 2-(2-chloroacetyl)-2,3,4,9-tetrahydro-1-[4-(methoxycarbonyl)phenyl]-1*H*-pyrido[3,4-*b*]indole-3-carboxylate (RSL3, a ferroptosis inducer) for different hours, and then subjected to staining with **V5** and CM-H2DCFDA, respectively. The establishment of ferroptosis in HCECs was confirmed using a lipid peroxidation fluorescence probe C11 BODIPY (Fig. S14 in Supporting information). As shown in Fig. S15 (Supporting information), obviously increasing viscosity was detected along with the ferroptosis processes. It has been verified that ferroptosis is tightly associated with the accumulation of lipid peroxides [58], and the staining results with CM-H2DCFDA confirmed the elevation of ROS level in HCECs after RSL3 treatment. Therefore, it is speculated

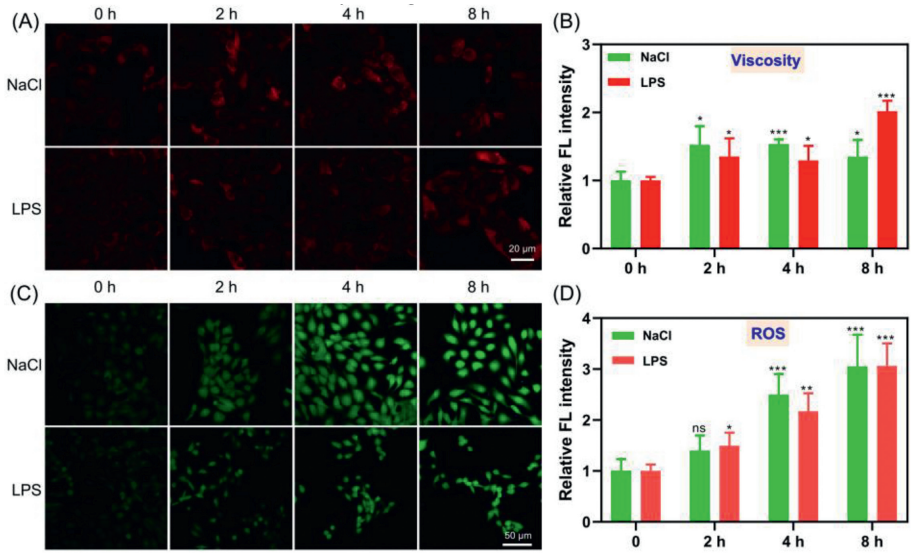

Fig. 2. HCECs were treated with NaCl (70 mmol/L) or LPS (1 μmol/L) for 0, 2, 4, or 8 h. Cells were then incubated with 5 μmol/L **V5** (A) or 10 μmol/L CM-H2DCFDA (C) for another 20 min before imaging. λ_{ex} = 488 nm, $\lambda_{em\text{-}\mathbf{V5}}$ = 570–620 nm, $\lambda_{em\text{-CM-H2DCFDA}}$ = 517–527 nm. (B, D) Quantitative statistical analysis of indicated fluorescence intensity in (A) and (C). $^{*}P < 0.05$, $^{**}P < 0.01$, $^{***}P < 0.001$; ns, no significance by Student's *T*-test. $n = 4$. Error bars are mean ± standard deviation (SD).

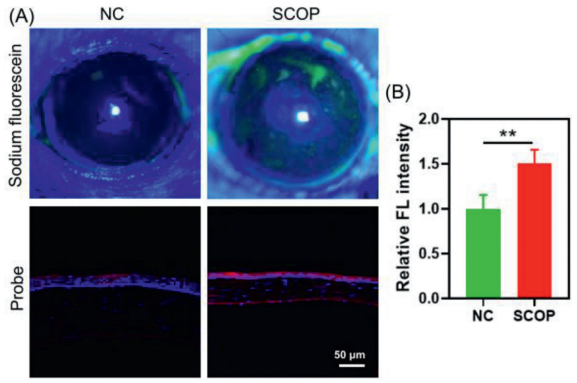

Fig. 3. (A) Up: staining of cornea in mice with sodium fluorescein; below: the corneal frozen sections from normal or SCOP-treated mice were incubated with **V5** (5 μmol/L) and DAPI for 20 min and then taken the confocal fluorescence images. λ_{ex} = 488 nm, λ_{em} = 570–620 nm. (B) Quantitative statistical analysis of fluorescence intensity for **V5**-stained corneal sections. $^{**}P < 0.01$ by Student's *T*-test. $n = 4$. Error bars are mean ± SD.

that the increasing viscosity during ferroptosis might be due to the accumulation of lipid peroxides. Thus, viscosity can serve as a useful target for the investigation of pathogenesis of DED in living cells mediated by various factors with the aid of a powerful fluorescent probe.

Finally, the probe was employed to image the viscosity changes in the corneal tissues from DED mice. DED mice were established by subcutaneous injection with scopolamine (SCOP, 2.5 mg/mL) 3 times a day for 5 consecutive days [59]. After the DED modeling, the staining of cornea in mice with sodium fluorescein (a clinical dye for indication of corneal integrity) showed obviously increasing fluorescence, suggesting the injury of corneal epithelial cells by SCOP (Fig. 3). In addition, phenol cotton thread test was employed to further confirm the DED modeling. As shown in Fig. S16 (Supporting information), apparent violet color was observed in the cotton thread from negative control (NC) group, while little color change was seen in that from SCOP group, suggesting the significantly reduced tear secretion of mice in SCOP group. In short, these results suggested the successful establishment of DED model in mice.

Afterwards, all mice were sacrificed for cervical dislocation. The fresh isolated mouse eyeballs were embedded in optimal cutting temperature compound and cut into sections with a thickness of 10 μmol/L. Corneal sections from normal mice served as NC. All tissues were stained with **V5** and 4′,6-diamidino-2-phenylindole (DAPI) before imaging. The cornea is divided into five layers, which from the outside to the inside are the corneal epithelial cell layer, the corneal proelastic layer, the corneal stroma layer, the corneal posterior elastic layer, and the corneal endothelial cell layer. It was clearly found that in NC group, strong blue fluorescence from DAPI was mainly observed in corneal epithelial cell layer with little red fluorescence from **V5** (Fig. 3). However, in SCOP group, stronger red fluorescence was visualized in the corneal epithelial cell layer and the corneal endothelial cell layer, suggesting a more viscous microenvironment in the corneal from DED mice. The results were consistent with those in HCECs. It should be noted that the thinner cornea in SCOP group is reasonable, because the core mechanism of dry eye is the apoptosis of corneal conjunctival epithelial cells caused by high osmotic pressure of tear, which leads to the thinning of total corneal thickness [52]. Therefore, probe **V5** is of potential in the imaging of varying viscosity in tissues from DED mice.

In conclusion, we constructed a fluorescent probe **V5** with an asymmetric D-A-D feature after rational structural modulation, and the probe manifests a remarkable fluorescence enhancement in highly viscous conditions without interferences from polarity and reactive species. It can selectively discriminate cancer cells from normal ones owing to their inherent higher viscosity. Furthermore, the probe is employed to monitor viscosity increment during DED progression in living cells and tissues. As a result, viscosity is suggested as an efficient indicator for DED pathology, and **V5** is the first probe used for monitoring DED-associated viscosity to the best of our knowledge. The underlying mechanism of viscosity changes during DED is under investigation in our group.

Declaration of competing interest

The authors declare that they have no known competing financial interests or personal relationships that could have appeared to influence the work reported in this paper.

Acknowledgments

This work was supported by the National Natural Science Foundation of China (No. 22075281), Zhejiang Provincial Natural Science of Foundation of China (No. LZ21B010001), and University of Chinese Academy of Science (No. WIUCASQD2020008).

Supplementary materials

Supplementary material associated with this article can be found, in the online version, at doi:10.1016/j.cclet.2023.108516.

References

[1] Z. Yang, J. Cao, Y. He, et al., Chem. Soc. Rev. 43 (2014) 4563–4601.
[2] L. Wang, Y. Xiao, W. Tian, L. Deng, J. Am. Chem. Soc. 135 (2013) 2903–2906.
[3] I. Lopez-Duarte, T.T. Vu, M. Izquierdo, J.A. Bull, M.K. Kuimova, Chem. Commun. 50 (2014) 5282–5284.
[4] W.J. Akers, M.A.J. Haidekker, Biomech. Eng. 127 (2005) 450–454.
[5] J. Lippincott-Schwartz, E. Snapp, A. Kenworthy, Nat. Rev. Mol. Cell Biol. 2 (2001) 444–456.
[6] J. Liu, W. Zhang, C. Zhou, et al., J. Am. Chem. Soc. 144 (2022) 13586–13599.
[7] A.E.G. Raine, Lancet 331 (1988) 97–100.
[8] L. Yu, J.F. Zhang, M. Li, et al., Chem. Commun. 56 (2020) 6684–6687.
[9] N. Wang, H. Wang, J. Zhang, et al., Chin. Chem. Lett. 33 (2022) 1584–1588.
[10] L. Zeng, T. Chen, B. Zhu, et al., Chem. Sci. 13 (2022) 4523–4532.
[11] S. Wang, L. Chen, P. Jangili, et al., Coord. Chem. Rev. 374 (2018) 36–54.
[12] S. Wang, B. Zhu, B. Wang, et al., Chin. Chem. Lett. 32 (2021) 1795–1798.
[13] H. Ye, S. Koo, B. Zhu, et al., Anal. Chem. 94 (2022) 15423–15432.
[14] Z. Xu, M.X. Zhang, Y. Xu, et al., Sens. Actuators B: Chem. 290 (2019) 676–683.
[15] L. Zeng, H. Zeng, L. Jiang, et al., Anal. Chem. 91 (2019) 12070–12076.
[16] W. Qu, W. Yuan, M. Li, Y. Chen, Chin. Chem. Lett. 32 (2021) 3837–3840.
[17] R. Zhang, L. Lian, B. Wang, et al., Spectrochim. Acta Part A 278 (2022) 121385.
[18] W. Sun, S. Guo, C. Hu, J. Fan, X. Peng, Chem. Rev. 116 (2016) 7768–7817.
[19] S. Wang, W.X. Ren, J.T. Hou, et al., Chem. Soc. Rev. 50 (2021) 8887–8902.
[20] J. Yin, L. Huang, L. Wu, et al., Chem. Soc. Rev. 50 (2021) 12098–12150.
[21] H. Xiao, P. Li, B. Tang, Chem. Eur. J. 27 (2021) 6880–6898.
[22] X. Yang, D. Zhang, Y. Ye, et al., Coord. Chem. Rev. 453 (2022) 214336.
[23] D. Su, C.L. Teoh, L. Wang, X. Liu, Y.T. Chang, Chem. Soc. Rev. 46 (2017) 4833–4844.
[24] C. Ma, W. Sun, L. Xu, et al., J. Mater. Chem. B 8 (2020) 9642–9651.
[25] A.Kung Tantipanjaporn, K.K.Y. Chan, et al., Sens. Actuat. B: Chem. 367 (2022) 132003.
[26] Y. Wu, C. Yin, W. Zhang, Y. Zhang, F. Huo, Anal. Chem. 94 (2022) 5069–5074.
[27] L. Chai, T. Liang, Q. An, et al., Anal. Chem. 94 (2022) 5797–5804.
[28] B. Dong, W. Song, Y. Lu, Y. Sun, W. Lin, ACS Sens. 6 (2021) 22–26.
[29] A. Zheng, H. Liu, X. Gao, K. Xu, B. Tang, Anal. Chem. 93 (2021) 9244–9249.
[30] J. Yin, X. Kong, W. Lin, Anal. Chem. 93 (2021) 2072–2081.
[31] S. Ye, H. Zhang, J. Fei, C.H. Wolstenholme, X. Zhang, Angew. Chem. Int. Ed. 60 (2021) 1339–1346.
[32] Y.N. Wang, B. Xu, L.H. Qiu, et al., Sens. Actuators B: Chem. 337 (2021) 129787.
[33] T. Mukherjee, R.J. Martinez–Sanchez, K.T. Fam, et al., Mater. Chem. Front. 5 (2021) 2459–2469.
[34] Y. Zhang, Q. Zhou, Y. Bu, et al., Anal. Chim. Acta 1178 (2021) 338847.
[35] S. Wang, B. Zhou, N. Wang, et al., Chin. Chem. Lett. 31 (2020) 2897–2902.
[36] L. Tang, L. Zhou, X. Yan, et al., Dyes Pigm. 182 (2020) 108644.
[37] M. Ren, Q. Xu, S. Wang, L. Liu, F. Kong, Chem. Commun. 56 (2020) 13351–13354.
[38] X. Liu, W. Chi, Q. Qiao, et al., ACS Sens. 5 (2020) 731–739.
[39] C. Liu, T. Zhao, S. He, L. Zhao, X. Zeng, J. Mater. Chem. B 8 (2020) 8838–8844.
[40] D. Han, J. Yi, C. Liu, et al., Spectrochim. Acta A 238 (2020) 118405.

[41] Y. Zhang, Z. Li, W. Hu, Z. Liu, Anal. Chem. 91 (2019) 10302–10309.
[42] H. Li, W. Shi, X. Li, et al., J. Am. Chem. Soc. 141 (2019) 18301–18307.
[43] L.L. Li, K. Li, M.Y. Li, et al., Anal. Chem. 90 (2018) 5873–5878.
[44] Z. Yang, Y. He, J.H. Lee, et al., J. Am. Chem. Soc. 135 (2013) 9181–9185.
[45] X. Wu, R. Wang, N. Kwon, H. Ma, J. Yoon, Chem. Soc. Rev. 51 (2022) 450–463.
[46] J.T. Hou, K.K. Yu, K. Sunwoo, et al., Chem 6 (2020) 832–866.
[47] M. Wang, X. Han, X. Yang, et al., Analyst 146 (2021) 6490–6495.
[48] L. Long, W. Liu, P. Ruan, et al., Anal. Chem. 94 (2022) 2803–2811.
[49] C. Yin, F. Huo, J. Zhang, et al., Chem. Soc. Rev. 42 (2013) 6032–6059.
[50] J. Mei, N.L.C. Leung, R.T.K. Kwok, et al., Chem. Rev. 115 (2015) 11718–11940.
[51] X. Wang, L. Fan, S. Wang, et al., Anal. Chem. 93 (2021) 3241–3249.
[52] F. Stapleton, M. Alves, V.Y. Bunya, Ocul. Surf. 15 (2017) 334–365.
[53] S. Barabino, Y. Chen, S. Chauhan, R. Dana, Prog. Retin. Eye Res. 31 (2012) 271–285.
[54] R. Yang, F. Meng, G. Niu, et al., Sens. Actuat. B: Chem. 372 (2022) 132639.
[55] M. Dogru, T. Kojima, C. Simsek, K. Tsubota, Invest. Ophthalmol. Vis. Sci. 59 (2018) DES163–DES168.
[56] R. Magny, K. Kessal, A. Regazzetti, et al., Biochim. Biophys. Acta Mol. Cell Biol. Lipids 1865 (2020) 158728.
[57] Y. Wei, P.A. Asbell, Eye Contact Lens 40 (2014) 248–256.
[58] X. Zuo, H. Zeng, B. Wang, et al., Invest. Ophthalmol. Vis. Sci. 63 (2022) 3.
[59] F. Peng, D. Jiang, W. Xu, et al., Invest. Ophthalmol. Vis. Sci. 63 (2022) 18.